PRAMANA
—journal of
physics

Vol. 50, No. 5,
May 1998
pp. 433–445

An electrostatic charge state selector for ion-atom collisions: Design, spectral line-shapes and performance

AMAL K SAHA, K V THULASI RAM, L C TRIBEDI, W A FERNANDES, S D NARVEKAR, V NANAL[1], M B KURUP, K G PRASAD[2] and P N TANDON
Tata Institute of Fundamental Research, Homi Bhabha Road, Colaba, Mumbai 400 005, India
[1]Present address: Argonne National Laboratory, Argonne, Illinois 60439, USA
[2]Present address: H-316, Vaishali Garden Apartments, Tarnaka, Secunderabad 500 017, India
Email: amal@tifr.res.in

MS received 12 February 1998

Abstract. An electrostatic charge state selector has been constructed for charge transfer studies in ion atom collisions. Its design and performance have been discussed illustrating with examples of some data taken using heavy ion beams from the pelletron accelerator. Expressions for the determination of charge state fractions from the observed charge spectrum in voltage scanning mode of operation and also the line shapes have been discussed analytically in detail.

Keywords. Ion-atom collision; charge state fractions; electrostatic charge state selector; spectral line-shapes.

PACS Nos 39.90; 34.70; 34.50

1. Introduction

In ion-atom collisions several single or multi-electron transfer processes occur between the projectile and the target atoms resulting invariably in a change of the charge carried by the incident ion. It is often required to associate the observable event in the collision process to the corresponding charge state of the ion after the collision has taken place. Thus analysis of the charge state of the ion after the collision becomes necessary. The final charge state information on the ion also provides vital information in some special cases. In the case of energetic heavy ions channeled through a thin crystal, for example, the 'frozen' fraction of the incident charge state is an important parameter in deriving capture cross sections (see e.g. ref. [1]). In recent years our group has undertaken a series of investigations concerning various aspects of ion-atom collisions in a solid target. A charge state selector was required to resolve the charge states of the ion after the collision process. We describe here the construction of a simple electrostatic charge state selector and illustrate its performance with examples of some of the data taken using BARC–TIFR pelletron accelerator. Analytical derivations of the possible line-shapes of the charge spectrum and procedure for the determination of the fractions of particles of different charge states from the observed spectrum are also presented.

2. Design details

The electrostatic charge state selector consists of two deflector plates to which a dc voltage up to ±50 kV could be applied. One of the plates was arranged at an inclination with respect to the other in order to avoid restrictions imposed by the parallel plate geometry thus effectively achieving higher charge dispersion than in a parallel plates arrangement. The plates were mounted in such a way that a positively charged particle is deflected in the vertical direction. The deflector electrodes were made from highly polished 74.5 cm long, 30 mm wide, and 0.5 cm thick SS plates. The distance between the plates was maintained to be 16 mm and 42 mm at the entrance and exit, respectively, by means of three sets of appropriately machined ceramic insulators. A drift space of 51 cm, which also accommodated the pumping system, was kept between the exit of the deflector plates and the Faraday cup. The vertically deflected ions were collected in a electron suppressed Faraday cup placed just behind a 2 mm high and 10 mm wide slit kept at a vertical distance of 45 mm from the undeflected beam position. A slit 1.5 mm wide and 10 mm high was placed at the entrance of the charge state selector to restrict the acceptance angle of the beam. A line drawing of the charge selector assembly is shown in figure 1. The high voltage on the plates was provided by a shielded cable which was connected via specially made high vacuum teflon feed-throughs (figure 2). The Faraday cup, behind the slits, was directly fitted to a standard vacuum feed-through which was also electrically isolated. Two externally programmable high voltage supplies were employed for providing the required voltages to the plates.

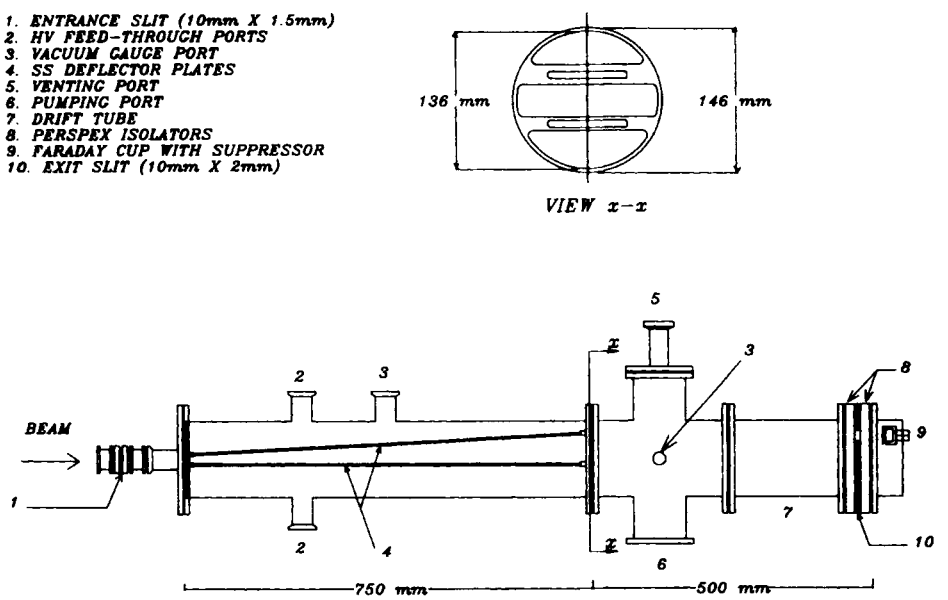

Figure 1. A line drawing of the charge state selector.

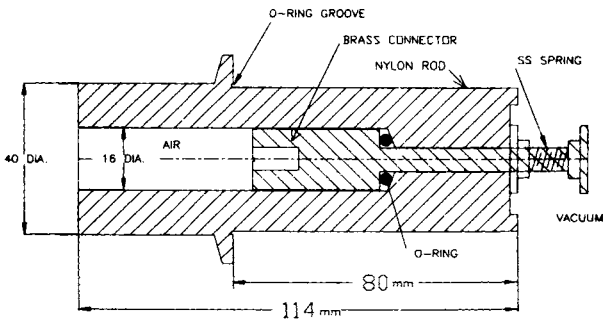

SECTIONAL VIEW OF
HIGH VOLTAGE FEED-THROUGH

Figure 2. Details of the high voltage feed-through.

3. Control and data collection

3.1 *Modes of operation of the charge state selector*

The charge spectra can be obtained either by recording the spectra at a fixed plate voltage in conjunction with a position sensitive particle detector at the exit of the charge selector (to be incorporated in near future) or, as is done in the present case, by recording the charge transmitted through a narrow vertical slit kept at a fixed distance, as a function of the plate voltage. Let us call the first mode of operation, PSD mode and the present one, voltage scanning (VS) mode. In VS mode, the charge is collected via a specially designed Faraday cup, kept just behind the slit. The charge collected by the Faraday cup is measured using an electrometer whose output was digitized. For incident charge normalization, the electrons emitted by the rotating wire of a beam profile monitor (BPM) mounted before the scattering chamber were collected and measured in similar way by another electrometer. This arrangement was particularly suitable while using very small currents which are inevitable in the case of fully stripped ions.

3.2 *Hardware*

In order to vary the voltage on the plates of the charge selector in finite steps and collect the data at each step, a PC based system was designed. Figure 3 shows the flow chart and the functional block diagram of the control and data collection system.

The interface (I/F) board consists of address, data and control signal buffer ICs, (2 × 74 ALS 244, 74 ALS 245), an address decoder (74 ALS 138), magnitude comparator 74LS6881, two 8255 programmable peripheral I/O devices, two 8254 count down counter ICs, a 10 bit D/A converter (AD561J) along with a fast settling time ($\sim 5\,\mu s$) operational amplifier (LF396) along with a sample and hold amplifier (LF 398). The buffered address lines, BA5 to BA9, are used to select the group address (300 Hex in our case), while the lines BA2–BA4 are used to derive chip select lines (maximum of 8 chips) on the I/O board. The function of the peripheral ICs to be carried out is determined using

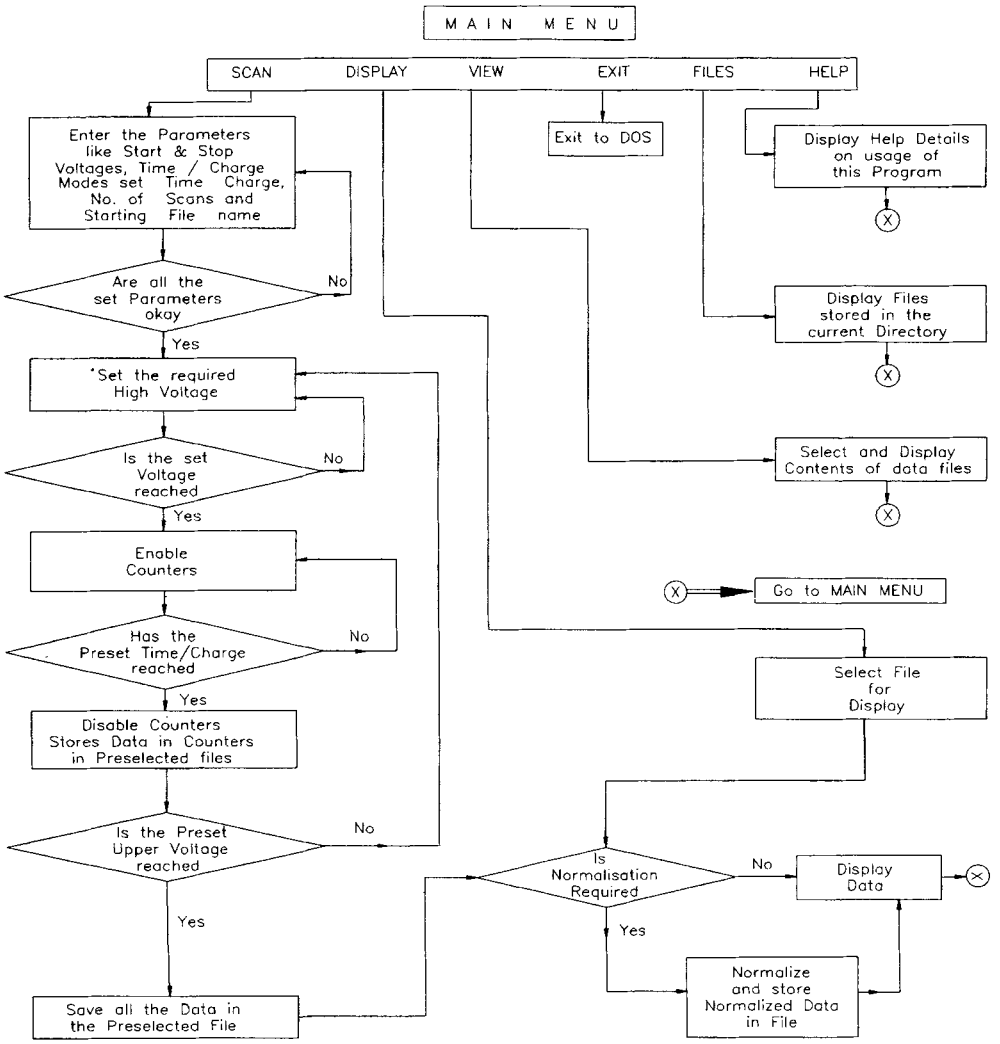

Figure 3. Flow chart and the functional block diagram of the control and data collection system of the charge state selector.

address lines BA0 and BA1. Each of the two 8255 ICs on the I/F board has three ports (A, B and C). One of the 8255 (CS1) is used to operate the D/A converter (8 bits of port A and 2 bits of port B together form 10 bits to drive the DAC). The output from the DAC is given to the operational amplifier LF 356, which gives a +ve output in the range of (0–5 V) or (0–10 V) selectable by a dip switch. An inverter is provided for −ve analog voltages of the same range. A sample and hold (S/H) amplifier serves to generate a steady DC signal for driving the programmable HV supplies. The functions of the S/H amplifier are: (i) to isolate the output signal from the input signal while the input bits of DAC are changing (ii) to wait for output voltage of LF 356 to settle down, thus giving a

steady final O/P voltage. The control logic signal for the S/H amplifier is obtained from Port C of the 8255 (CS1). A selective O/P voltage limiter and safety electronic switch is incorporated for limiting the high voltage on the plate to a safe level. This also protects the high voltage supply from software mistakes and hardware faults which would lead to full 50 kV on each plate causing sparks. We have provided one more 8255 (CS0) for control and operation of other devices (like stepper motors etc.) in future.

In order to collect data from various devices like Faraday cups, detectors, current integrators, timers etc., six 16 bit count down counters are provided using two 8254 ICs (CS2 and CS3). As soon as the plate voltage is set, the counters are loaded with maximum count length (max value of 16 bits) and are enabled. These counts are down counted. The data is fed at the i/p of each counter in the form of serial TTL pulses. After a preset time or counts is reached, the counters are disabled, the data from the counters are read to obtain the actual counts and stored in files. All the data IN and OUT are transferred using the buffered data lines BD0–BD7. The read and write instructions from the PC are given by the BIOR and BIOW lines through the decoder. Simultaneously, the plate voltage is incremented to the next value and the cycle is repeated. The counters are enabled or disabled using the PC1 and PC0 lines of the port C of the first 8255 (CS1) device. After the data collection at the highest preset value of the plate voltage, the complete data is transferred to a previously named file in the PC. Also the data from counters 1 and 3 are displayed on the monitor. It is also possible to interactively normalize the data of counter 3 to the corresponding data counter 1 and display the normalized data. The whole set of data collection with same parameter can be repeated interactively by a single key.

3.3 *Software*

A user friendly menu driven interactive software using 'Basic' was written. This software provides several options, which are briefly described below:

Scan: Using this option the plate voltages (both positive and negative) can be set to vary simultaneously with a common control between two limits in finite steps. Six set of charge data collected on various slits, FC etc. or particles detected in the counters can be recorded at each step for a given time interval or for a preset number of incident particles. Once the selected voltage scan is completed, the number of contents of the two counters are displayed as a function of the applied voltage. Simultaneously, the data from all counters are stored in a file. The data of one of the counters could be normalized with respect to the other counter at each voltage step and can be viewed. The scan with same input parameters can be repeated several times either automatically or interactively.

Display: This option allows the data of two files stored earlier to be displayed.

View: In this option the data from all counters recorded earlier in a file along with various parameters used are displayed on the monitor screen of the PC.

Files: Various files existing in a directory can be viewed using this option.

Help for Menu: This option describes the details of various options in the menu.

Exit: This option closes all the open files and exits from the program to DOS shell of the PC.

4. Spectral line shapes and charge state fractions

It can be shown that in the inclined plate geometry the total vertical deflection s of the beam of charge q and energy E in the plates of length l and a drift region l_{drift} can be expressed as

$$s = y_{\text{inc}} + (l + l_{\text{drift}}) \tan \alpha_{\text{inc}} + \frac{qV}{2E} \frac{l^2}{d_e - d_0} \left[\left\{ \frac{d_e}{d_e - d_0} + \frac{l_{\text{drift}}}{l} \right\} \ln \left(\frac{d_e}{d_0} \right) - 1 \right], \tag{1}$$

where V is the applied voltage difference between the plates and d_0 and d_e are the distances between the plates of the charge selector at the entrance and exit, respectively. y_{inc} is the transverse displacement of the charged particle from the optic axis and α_{inc} is the angle of incidence with respect to the optic axis. Let us introduce the constants C_1 and C_2 so that s can be expressed as

$$s = y_{\text{inc}} + C_1 \tan \alpha_{\text{inc}} + C_2 \left(\frac{qV}{E} \right). \tag{2}$$

C_1 and C_2 are functions of the geometrical parameters of the charge state selector only. The deflection s can be obtained directly in mm when one expresses l, d_e, d_0, and l_{drift} in mm, the projectile energy E in MeV, the voltage V in kilo-Volts and the projectile charge q in eletronic unit.

As already mentioned, the charge state of the incident ion may change during the collision with the target atoms and a distribution of charge states is produced after the collision. In this section we derive the fractions of post-collision charge states which enter the selector and also their spectral line shapes.

Typical charge spectra normalized to the number of ions incident on the target are shown in figures 4, 5 and 7. In the absence of any spread in the transverse position and the angle of the beam, the charge spectrum would have been a step function of the applied plate voltage (V). It is the distribution of transverse position and the angular spread of the beam with respect to the exit slit that determines the shape of the spectrum. In the PSD mode of operation, the spectrum would be the exact map of the distribution of transverse position of the particles. In the voltage scanning mode, however, at each voltage point, a position integral, between the edges of the exit slit, of the position distribution of the beam on the exit slit plane is obtained. It should be noted that there is always some overlap in the integrals of the position distribution at successive voltage points. One needs, therefore, to deconvolute the voltage mode spectrum to find the fraction of particles of different charge states.

Let us assume that there are particles of different charge states q's passing through the charge selector. Let N_q be the number of particles of charge state q entering the selector at any plate voltage. In the voltage mode charge spectrum, $F(V)$ is the total charge passing through the exit slit at the applied plate voltage V and collected by the Faraday cup behind the exit slit.

If f_q (V) be defined as the contribution of particles of charge state q to the total charge $F(V)$ at the voltage point V, then

$$F(V) = \sum_q f_q(V). \tag{3}$$

Let α_{inc} and y_{inc} be the angle of incidence and the displacement from the optic axis, respectively, of the incident ions. The distribution of α_{inc} and y_{inc} is assumed to be independent of the charge state q since it is caused mainly by the Rutherford scattering of the ion with the nuclei of the atoms that lie on its way to the charge selector.

Let $p(y_{inc}, \alpha_{inc})$ be the probability density function describing the charge independent distribution of the divergence parameters y_{inc} and α_{inc}.

$$f_q(V) = \int\int\int q \cdot N_q \cdot \mathrm{d}y_{inc}\, \mathrm{d}\alpha_{inc}\, p(y_{inc}, \alpha_{inc})\mathrm{d}s \times \delta\left(s - \left(y_{inc} + C_1 \tan\alpha_{inc} + C_2 \frac{qV}{E}\right)\right) W(s), \tag{4}$$

where

$$W(s) = \theta(s - s_1) - \theta(s - s_2) \tag{5}$$

is the window function representing the exit slit with edges at s_1 and s_2, $s_2 > s_1$. Here

$$\theta(x) = 1 \quad \text{if } x > 0$$
$$= 0 \quad \text{otherwise.}$$

Therefore, by change of variable $u = C_2(qV/E)$

$$\int f_q(V)\mathrm{d}V = qN_q \int\int\int\int \mathrm{d}y_{inc}\, \mathrm{d}\alpha_{inc}\, \mathrm{d}V\, \mathrm{d}s\; p(y_{inc}, \alpha_{inc}) W(s) \times \delta\left(s - \left(y_{inc} + C_1 \tan\alpha_{inc} + C_2 \frac{qV}{E}\right)\right) \tag{6}$$

$$= \frac{EqN_q}{C_2 q} \int\int\int\int \mathrm{d}y_{inc}\, \mathrm{d}\alpha_{inc}\mathrm{d}s\, \mathrm{d}u\; p(y_{inc}, \alpha_{inc}) W(s) \times \delta(s - (y_{inc} + C_1 \tan\alpha_{inc} + u)). \tag{7}$$

And

$$\int f_q(V)\mathrm{d}V = \frac{EN_q}{C_2} I, \tag{8}$$

where

$$I \equiv \int\int\int\int \mathrm{d}y_{inc}\, \mathrm{d}\alpha_{inc}\, \mathrm{d}s\, \mathrm{d}u\; p(y_{inc}, \alpha_{inc}) W(s) \delta(s - (y_{inc} + C_1 \tan\alpha_{inc} + u)). \tag{9}$$

The value of the integral I is independent of the charge state and depends only on $p(y_{inc}, \alpha_{inc})$ and the geometrical constants of the charge selector.

By similar change of variable, it is easy to show that (for a given energy)

$$\int f_q(V) g(qV)\mathrm{d}V = kN_q, \tag{10}$$

$$g(qV) = \text{any function of } qV, \tag{11}$$

$$k = \text{constant independent of } q. \tag{12}$$

The area under the individual charge profile $f_q(V)$ in VS mode i.e. $\int f_q(V)\mathrm{d}V$ is proportional to N_q and is *not* proportional to qN_q as a cursory look into the problem might have suggested. The charge state fractions i.e. $N_q/\sum_q N_q$ can therefore be obtained directly from the areas under the peaks for different charge states. It may be noted that in PSD mode, the area under individual charge profile obtained by integrating the profile over the variable s would also be proportional to N_q.

In the special case of Gaussian distribution

$$p(y_{\mathrm{inc}}, \alpha_{\mathrm{inc}}) = \frac{1}{\sqrt{2\pi\sigma^2_{\alpha_{\mathrm{inc}}}}} \exp\left[-\frac{\alpha^2_{\mathrm{inc}}}{2\sigma^2_{\alpha_{\mathrm{inc}}}}\right] \frac{1}{\sqrt{2\pi\sigma^2_{y_{\mathrm{inc}}}}} \exp\left[-\frac{y^2_{\mathrm{inc}}}{2\sigma^2_{y_{\mathrm{inc}}}}\right], \tag{13}$$

it can be shown by explicit evaluation of the integral that

$$f_q(V) = qN_q \frac{1}{2}\left[\mathrm{erf}\left(\frac{s_2 - C_2\frac{qV}{E}}{\sqrt{\sigma^2_{y_{\mathrm{inc}}} + \sigma^2_{\alpha_{\mathrm{inc}}} C_1^2}}\right) - \mathrm{erf}\left(\frac{s_1 - C_2\frac{qV}{E}}{\sqrt{\sigma^2_{y_{\mathrm{inc}}} + \sigma^2_{\alpha_{\mathrm{inc}}} C_1^2}}\right)\right]. \tag{14}$$

It is worth investigating two limits of the above results.

I. *Narrow exit window*: When $(s_2 - s_1) \ll \sqrt{\sigma^2_{y_{\mathrm{inc}}} + \sigma^2_{\alpha_{\mathrm{inc}}} C_1^2}$,

$$f_q(V) = \frac{qN_q}{2} \frac{(s_2 - s_1)}{\sqrt{\sigma^2_{y_{\mathrm{inc}}} + \sigma^2_{\alpha_{\mathrm{inc}}} C_1^2}} \frac{1}{\sqrt{2\pi}} \cdot \exp\left[-\frac{\left(V - \frac{s_1+s_2}{2}\frac{E}{C_2 q}\right)^2}{2\left(\frac{E\sqrt{\sigma^2_{y_{\mathrm{inc}}} + C_1^2\sigma^2_{\alpha_{\mathrm{inc}}}}}{C_2 q}\right)^2}\right]. \tag{15}$$

That is, $f_q(V)$ is a Gaussian with peak at

$$V_q = \frac{s_1 + s_2}{2}\frac{E}{C_2 q} \tag{16}$$

and

$$\mathrm{FWHM} = 2.35\ \frac{E\sqrt{\sigma^2_{y_{\mathrm{inc}}} + C_1^2\sigma^2_{\alpha_{\mathrm{inc}}}}}{C_2 q}. \tag{17}$$

It may be noted that the peak height of $f_q(V)$ is proportional to qN_q with the constant of proportionality being equal for all the charge states. So the peak heights can also be used to find the charge state fractions.

II. *Wide exit window*: When $(s_2 - s_1) \gg \sqrt{\sigma^2_{y_{\mathrm{inc}}} + \sigma^2_{\alpha_{\mathrm{inc}}} C_1^2}$,

$$f_q(V) = qN_q \quad \text{at } V \text{ around } V_q \equiv \left(\frac{s_1 + s_2}{2}\right) \cdot \frac{E}{C_2 q} \tag{18}$$

$$= 0 \quad \text{for } |V - V_q| \gg \frac{E\sqrt{\sigma^2_{y_{\mathrm{inc}}} + C_1^2\sigma^2_{\alpha_{\mathrm{inc}}}}}{C_2 q}. \tag{19}$$

So it is a step function in V.

5. Performance of the charge selector

5.1 *Experimental setup*

The performance of the charge selector was checked using a setup discussed in our earlier papers [1, 2]. Briefly, a highly collimated beam of energetic heavy ions in a given charge state obtained from the 14 MV pelletron accelerator at Mumbai was made to fall on a target mounted inside an electrically isolated scattering chamber. In some cases the ions were further stripped using a post accelerator foil stripper [3]. The targets used were thin carbon foils of varying thicknesses mounted on a target wheel [4]. The scattered beam at 0° entered the charge selector through an isolated vertical $1.5 \times 12\,mm^2$ slit, mounted just before the plates. The charge state distribution of the scattered beam was measured by deflecting it as a function of the voltage on the plates. The deflected beam, transmitted through a horizontal slit 10×2 mm, was collected on a Faraday cup. A beam profile monitor, placed before the scattering chamber, was used to normalize the charge of the incident beam by measuring the number of emitted electrons from the BPM cathode wire. All the charge collected were digitized using AD converters which were specially designed and made such that they could be used even when the incident beam intensity is very low in the measurement. Since the AD converters were sensitive to only one polarity, a dc offset was helpful in averaging out small negative pickup by the electrometer. The charge spectra as a function of the plate voltage were recorded several times for a particular incident charge state and energy. They were normalized for a fixed incident charge for further analysis.

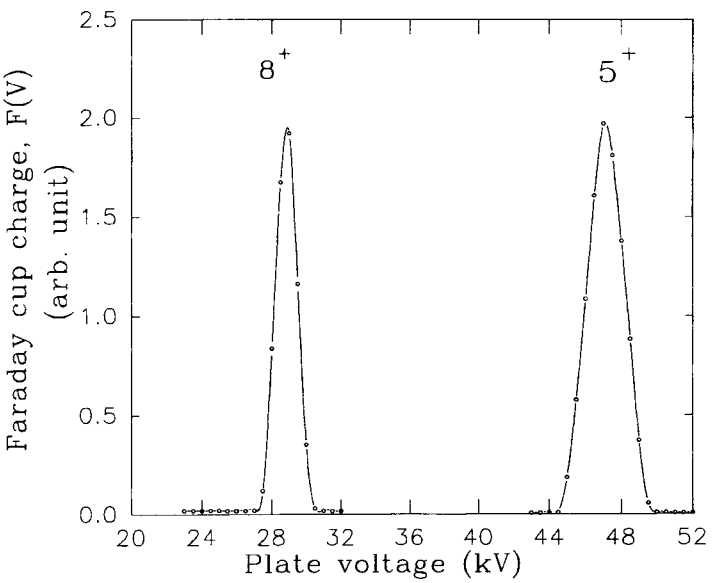

Figure 4. Typical charge spectra in VS mode normalized to the number of incident 60 MeV F ions. The spectra were taken separately with two different charge states (5^+ and 8^+).

5.2 *Performance*

The performance of the charge selector was tested using energetic ions in single or several charge states. The former was achieved by selecting a desired charge state either by direct acceleration or by allowing the beam to go through a post-stripper [4] and

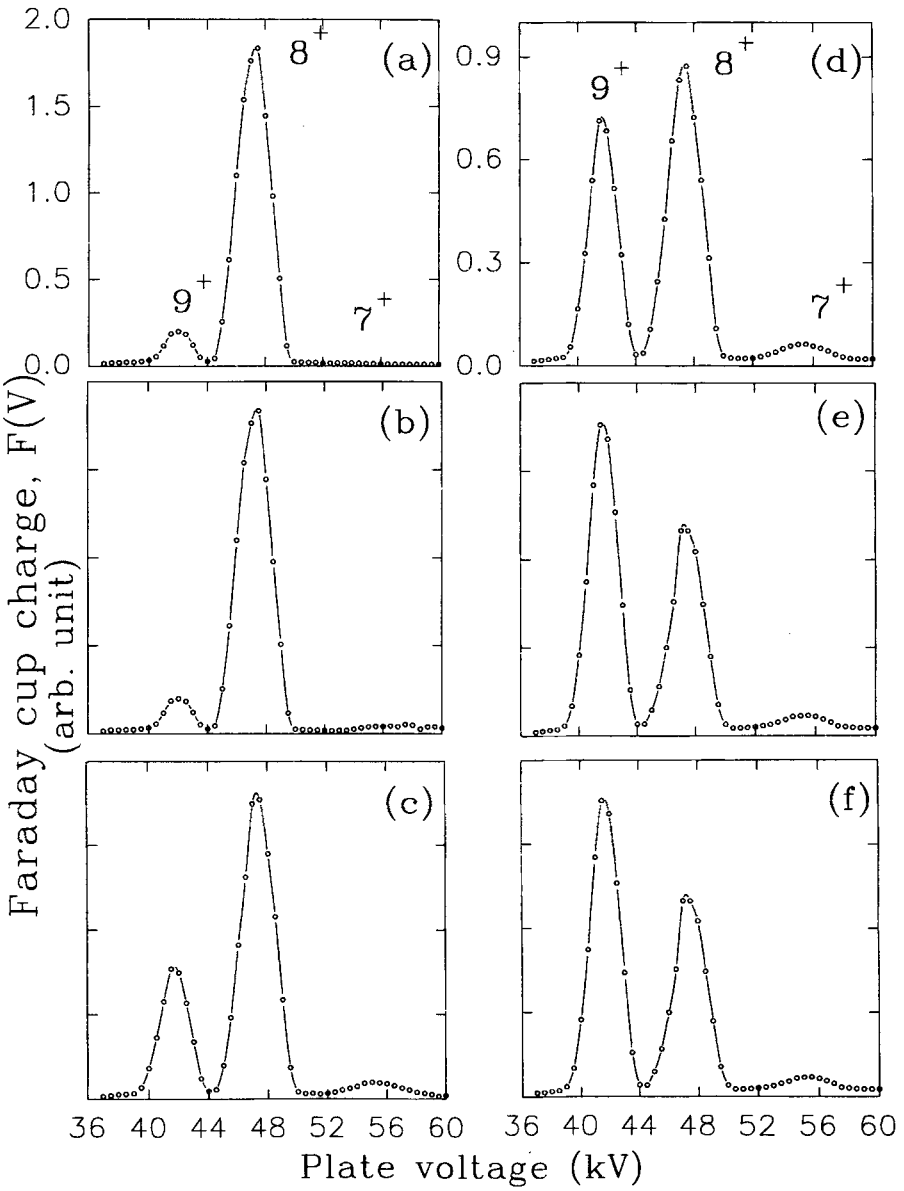

Figure 5. Normalized charge spectrum as in figure 4 with 96 MeV F^{8+} ions incident on C foil of thickness: (**a**) 1.5, (**b**) 2, (**c**) 5, (**d**) 10, (**e**) 20 and (**f**) 30 $\mu g/cm^2$.

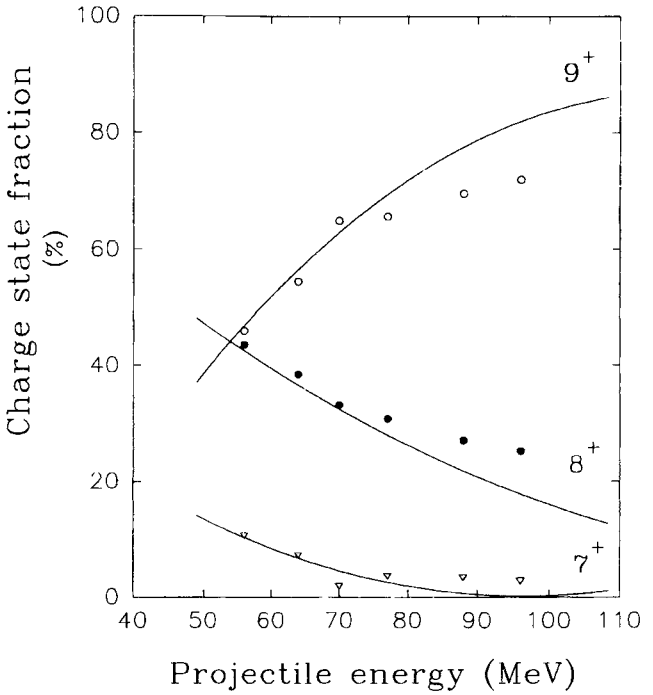

Figure 6. Charge state fractions obtained from the spectra taken with the charge state selector for F^{8+} ion incident on 30 μg/cm^2 C foil as a function of energy of the projectile. The solid curves are results reported by Shima *et al* [5].

subsequently selecting the desired charge state by a switching magnet. For obtaining several charge states to go through the selector the beam was passed through a set of carbon foils of varying thickness between 1.5 and 30 μg/cm^2. Any one of the carbon foil could be brought onto the path of the beam by remote control. Some positions on the holder were left blank in order to allow ions in a definite charge state to enter the selector. Typical charge profiles obtained at the Farady cup with a 5^+ or 8^+ charge state of the incident beam are shown in figure 4 for 60 MeV F ions. The latter was obtained with the help of the post stripper foils. The observed line shape is Gaussian. The resolution in VS mode, $\Delta V/V$ where ΔV is the FWHM of the profile and V is the voltage at which the peak appears, was found to be $\sim 5.3\%$ in the present geometry for both the cases suggesting that the inherent beam quality (emittance, focussing and stripping elements) to be the deciding factor. In cases where the beam enters the selector through a carbon foil placed before the selector, because of the Coulomb interaction, the beam is split into several charge states. The charge state fractions thus obtained depend not only on the incident energy and the atomic number of the ion beam but to a significant extent on the thickness of the carbon foil used until charge equilibrium is attained (before equilibrium is reached these fractions may also depend on the incident charge state). This is nicely illustrated in figure 5 which shows the observed charge spectra for several thicknesses of carbon foil for 96 MeV F ions. One can see a gradual increase in the 9^+ charge state fraction as the thickness of the foil increases signifying that charge equilibrium has not been

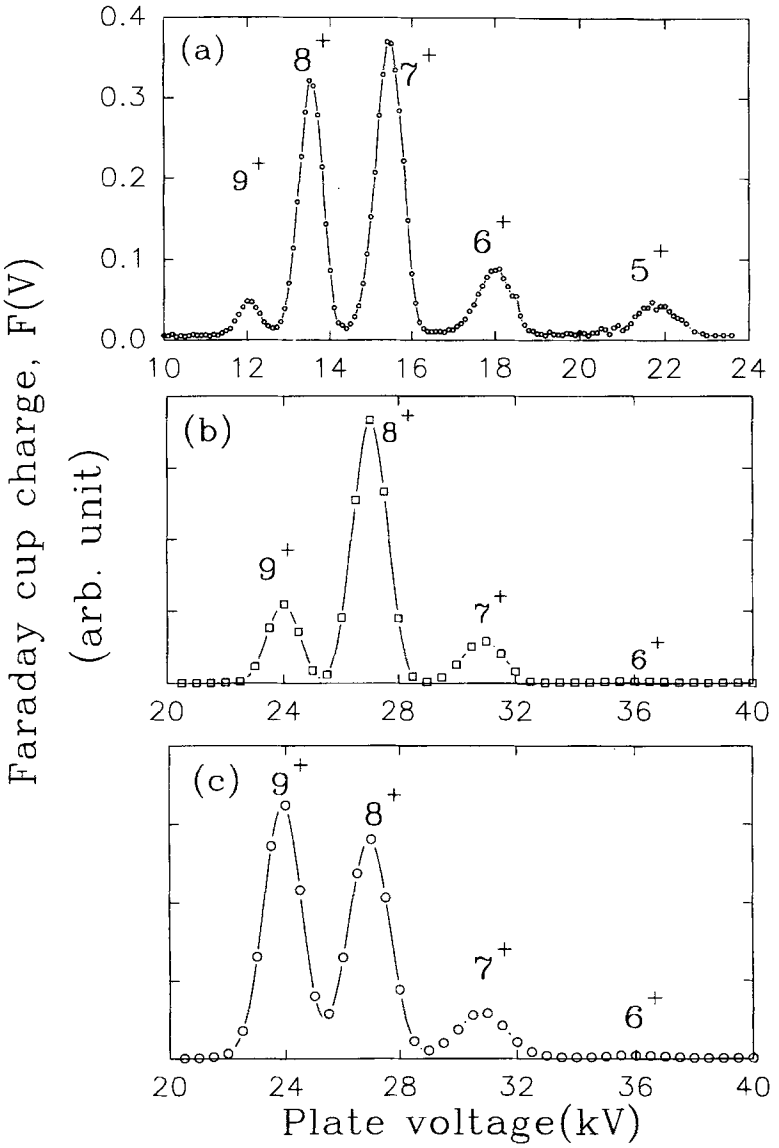

Figure 7. Normalized charge spectra, as in figure 4, with a beam of: (**a**) 24 MeV F^{8+} (obtained using gas stripper) incident on 3 $\mu g/cm^2$ C foil, (**b**) 56 MeV F^{8+} (obtained using foil stripper) incident on 3 $\mu g/cm^2$ C foil and (**c**) 56 MeV F^{8+} (obtained using foil stripper) incident on 30 $\mu g/cm^2$ C foil.

reached. From a fit to the spectra with Gaussian line shape the charge state fractions were determined (see IV). We have shown in figure 6, as a function of the incident beam energy, the charge state fractions obtained with a 30 $\mu g/cm^2$ C foil. As expected, the 9^+ fraction is found to increase with the beam energy. This figure also shows as solid lines

similar data reported by Shima *et al* [5], however, using a much thicker C foil of thickness 132 $\mu g/cm^2$. These lines are obtained by joining the experimental data points of Shima *et al*. Our low energy data (below 70 MeV) are found to be in very good agreement with that of Shima *et al*. However, as seen from the higher energy data, it is evident that charge equilibrium is not achieved with the 30 $\mu g/cm^2$ C foil used by us. The presently observed deviations at higher energies are expected to disappear had we used thicker foils. Such measurements would result in an increase of the 9^+ fraction with a corresponding decrease in the 8^+ and 7^+ fractions. The effect of the increased divergence of the beam due to the thickness of the C foil arising mainly due to multiple scatterings can be seen in figure 7 for F ions of 56 MeV. A comparison of the charge spectra taken with 3 and 30 $\mu g/cm^2$ foils (figures 7b and 7c) indicates the broadening of the lines caused mainly by Rutherford scattering. This is not so obvious at higher energy of 96 MeV (figure 5) where this contribution is small. Figure 7a shows the charge spectrum with 24 MeV F^{8+} obtained using gas stripper in the terminal of the accelerator to have a beam with smaller divergence. The charge spectrum taken with a 3 $\mu g/cm^2$ C foil is still very well resolved even though one expects larger line-widths due to Rutherford scattering because of the still lower energy suggesting that the beam quality before the scattering chamber is the principal factor deciding the resolution.

6. Conclusion

An electrostatic charge selector for charge state analysis has been constructed and its performance tested. The data obtained using this selector on charge state fractions of F ions after interacting with C foil are found to be in good agreement with the published data of Shima *et al* [5]. The effect of beam divergence on the experimental spectral line-width is well parametrized by the analytical expressions presented here.

Acknowledgement

The authors acknowledge useful discussion on spectral line shapes and charge state fractions with R G Pillay and A A Tulapurkar.

References

[1] L C Tribedi, V Nanal, M B Kurup, K G Prasad and P N Tandon, *Phys. Rev.* **A51**, 1312 (1995)
[2] L C Tribedi, K G Prasad and P N Tandon, *Phys. Rev.* **A47**, 3739 (1993)
[3] S D Narvekar, R R Hosangadi, L C Tribedi, R G Pillay, K G Prasad and P N Tandon, *Pramana – J. Phys.* **39**, 79 (1992)
[4] L C Tribedi, S D Narvekar, R G Pillay and P N Tandon, *Pramana – J. Phys.* **39**, 661 (1992)
[5] K Shima, T Mikumo and H Tawara, *Atomic Data Nucl. Data Tables* **34**, 357–391 (1986)